Electrocatalytic Water Oxidation by a Molecular Cobalt Complex through a High Valent Cobalt Oxo Intermediate

Debasree Das, Santanu Pattanayak, Kundan K. Singh, Bikash Garai and Sayam Sen Gupta*

Table of Contents

Physical measurements: ^{1}H NMR was performed in Bruker 400 and was reported in δ(ppm) *vs* (CH$_3$)$_4$Si with the deuterated solvent (CD$_3$CN) proton residuals as internal standard standards. The number of scans was kept 2000. HRMS (High Resolution Mass Spectroscopy) was done in Thermo Scientific Q-Exactive, using electron spray ionization source, Orbitrap as analyzer, connected with a C18 column (150 mm × 4.6 mm × 8 μm) and Maxis Impact (BRUKER) Sr no.282001.0008 respectively. Dissolved oxygen measurements during water oxidation (WO) were performed using a Clark type electrode (dissolved oxygen meter) from MicroSet (MS 0257), India, working in the range of 0 to 45 ppm with resolution of 0.01 ppm. Dynamic Light Scattering (DLS) analyses were run in Zetasizer Nano series Nano ZS90. For each set, solution pH was measured with a pH meter (LABINDIA, PICO+) with calibrated electrode with accuracy of ±0.2 pH. SEM (Scanning Electron Microscopy) imaging and EDX (Energy Dispersive X-ray spectroscopy) was recorded in a FEI Tecnai TF-20 instrument.

Details of Dissolved Oxygen measurement during CPE by using a Clark type electrode

In order to measure the evolved oxygen during CPE (controlled potential electrolysis) a Clark type electrode was used. The Clark electrode was previously calibrated before each experiment following a two point calibration 0% (zero solution) and 100% (air). CPE was performed in a four necked electrochemical cell. The electrochemical cell contained 1mM [Co^{III}-bTAML]$^-$ dissolved in 0.1 M pH = 9.2 phosphate buffer. An ITO electrode (1 cm^2) along with Ag/AgCl (satd) as reference and platinum wire as counter electrode was used for electrolysis. The Clark electrode was also fitted in the cell for measuring the dissolved oxygen. A solution of 0.1M pH = 9.2 phosphate buffer was used as supporting electrolyte. Before applying potential, the dissolved O$_2$ was completely removed from the buffer in the electrochemical cell by purging with high purity argon gas under slow stirring. Before applying potential the oxygen sensor displayed 0 ppm oxygen level. With the application of electrolysis potential (1.5V *vs* NHE), oxygen evolution was noted in the Clark electrode due

to increase in ppm level of oxygen in the electrochemical cell. CPE was carried out for 3 hours and oxygen evolution was monitored by Clark electrode. The results of the WO catalyzed by $[Co^{III}\text{-bTAML}]^-$ were compared with control experiment performed under the same conditions but in the absence of $[Co^{III}\text{-bTAML}]^-$. The Faradic efficiency was calculated according to the total charge passed (charge passed for control experiment was subtracted) during CPE and the total amount of evolved oxygen (considering WO as a 4 electron process).

Sample preparation for SEM and EDX experiment

The surface of a clean ITO slide (five times cleaned with water after sonication) was imaged for SEM and EDX analysis. The same ITO electrode was used during CPE for 3 hrs and then the ITO was rinsed carefully by Milli-pore water and then dried in high vacuum for 10-hrs. The dry surface was visualized under microscopy and the SEM image with its EDX report was compared with the results of clean ITO surface before CPE.

Details of Electrochemistry

Cyclic voltammetry experiments were carried out on a CHI-660 potentiostat. Glassy Carbon (GC) (3 mm of diameter), Silver/Silver chloride (saturated KCl salt), and Pt wire was used as working electrode, as reference electrode (unless explicitly mentioned) and counter electrode respectively. Before each measurement pre-treatment of the working electrode was done by polishing with 0.05 μm alumina paste, rinsing thereafter with water/acetone and finally blow-drying. Pre-treatment of the ITO electrodes were done by sonication in acetone, ethanol and Milli-Q ultrapure water sequentially for 10 min. All redox potentials in the present work are reported versus NHE by adding 0.19 V to the measured potential. $E_{1/2}$ values for the redox processes studied in this work are estimated from half of the sum of potential at the I_{max} of cathodic and anodic in CV measurements. IR compensation was done for the experiment where the buffer concentration was slowly increased in acetonitrile containing **2**. All other

kinds of measurements were done without IR compensation. When acetonitrile was used as organic solvent, 0.1M potassium hexafluorophosphate (KPF$_6$) was added as a supporting electrolyte and Ag/AgNO$_3$ (0.01M) was used as a non-aqueous reference electrode. All redox potentials (vs Ag/Ag$^+$) were reported to the values versus NHE by adding 0.5(unless explicitly mentioned).

Crystallographic Details

For the single Crystal X-ray diffraction experiment, as synthesized crystals of the respective materials were taken out of the solution and coated with Paratone-N oil. It was then placed in a nylon cryoloop (Hampton research) and then mounted in the diffractometer. The data collection was done at 298 K. The crystals were mounted on a Super Nova Dual source X-ray Diffractometer system (Agilent Technologies) equipped with a CCD area detector and operated at 250 W power (50 kV, 0.8 mA) to generate Mo Kα radiation (λ = 0.71073 Å) and Cu Kα radiation (λ = 1.54178 Å) at 298(2) K. Initial scans of each specimen were performed to obtain preliminary unit cell parameters and to assess the mosaicity (breadth of spots between frames) of the crystal to select the required frame width for data collection. CrysAlis^{Pro} [1] program software was used suite to carry out overlapping φ and ω scans at detector (2θ) settings (2θ = 28). Following data collection, reflections were sampled from all regions of the Ewald sphere to redetermine unit cell parameters for data integration. Following exhaustive review of collected frames, the resolution of the data set was judged. Data were integrated using CrysAlis^{Pro} software with a narrow frame algorithm. Data were subsequently corrected for absorption by the program SCALE3 ABSPACK scaling algorithm.

These structures were solved by direct method and refined using the SHELXTL 97[2] software suite. Atoms were located from iterative examination of difference F-maps following least squares refinements of the earlier models. Final model was refined anisotropically (if the

number of data permitted) until full convergence was achieved. Hydrogen atoms were placed in calculated positions (C-H = 0.93 Å) and included as riding atoms with isotropic displacement parameters 1.2-1.5 times U_{eq} of the attached C atoms. In some cases modeling of electron density within the voids of the frameworks did not lead to identification of recognizable solvent molecules in these structures, probably due to the highly disordered contents of the large pores in the frameworks. Highly porous crystals that contain solvent-filled pores often yield raw data where observed strong (high intensity) scattering becomes limited to ~1.0 Å at best, with higher resolution data present at low intensity. Additionally, diffused scattering from the highly disordered solvent within the void spaces of the framework and from the capillary to mount the crystal contributes to the background and the 'washing out' of the weaker data. Electron density within void spaces has not been assigned to any guest entity but has been modeled as isolated oxygen and/or carbon atoms. The foremost errors in all the models are thought to lie in the assignment of guest electron density. The structure was examined using the *ADSYM* subroutine of PLATON[3] to assure that no additional symmetry could be applied to the models. The ellipsoids in ORTEP diagrams are displayed at the 50% probability level unless noted otherwise.

Materials: All the materials used in this study were purchased from various commercial sources (Sigma Aldrich, Fisher Scientific etc). N, N dichloroformylmethylamine was obtained from ChemCollect, Gmbh. LCMS grade acetonitrile from Fisher was used. High purity Milli-Q water was used in all electrochemical study. All the solvents for synthesis were dried and purified as described elsewhere.[4] Indium tin oxide (ITO) electrode (8-10 ohm/sq) was obtained from global nanotech, India.

Synthesis of (Et₄N)[Co^III-bTAML]

Synthesis of the ligand (**L1**) was carried out by following the previously reported methodology for related teraammido macrocyclic ligand.[5]

A solution containing compound **L2** (X = H; 50 mg, 0.138 mmol) in 10 ml of dry terahydrofuran was deoxygenated. Then to this solution n-BuLi (0.4 ml of 1.4 M solution in hexane, 0.567 mmol, 4.1 equivalents) was added at 0 °C under Argon atmosphere followed by addition of 1.2 equivalents solid anhydrous cobalt(II)chloride under positive argon flow. The reaction was allowed to proceed under Argon at room temperature for overnight after which it was opened to air and stirred for one more hour to yield a dark purple brown precipitate. The precipitate was filtered through a frit funnel and was dissolved in methanol to afford a purple brown solution. The solution (5 ml) containing the complex was then loaded onto a cationic ion-exchange resin (Amberlite-120; strong acid) column that had been pre-saturated with tetraethyl ammonium ion so as to exchange the lithium counter cation. The purple band was eluted with methanol and the solvent was removed under reduced pressure to yield a purple solid**.** Further purification was achieved by column chromatography using basic alumina with dichloromethane: methanol = 99:1 as the eluent. X-ray diffracting quality crystals were obtained by slow vapor diffusion of diethyl ether into the solution of the complex in acetonitrile.
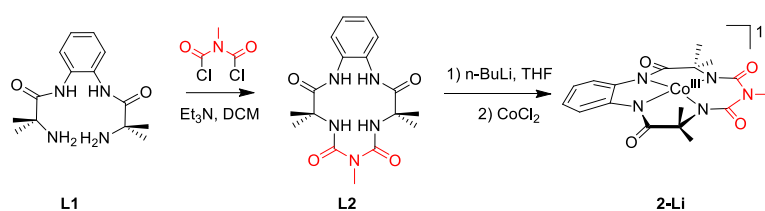
Scheme S1. Synthesis scheme of complex **2-Li.** Complex **2** was obtained as lithium counter cation

Synthesis of oxocobalt(IV)(bTAML)

By controlled potential electrolysis in acetonitrile

Complex **2** was dissolved in acetonitrile (0.1M KPF_6 used as supporting electrolyte) and bulk electrolysis was performed at -15°C using 9 cm^2 ITO electrode as the working electrode,

platinum foil as counter electrode and $Ag/AgNO_3$ as reference electrode. Low temperature UV-Vis spectra were recorded to detect the high valent cobalt oxo intermediates.

By using chemical oxidant (ceric ammonium nitrate) in acetonitrile and dichloromethane

Complex **2**(0.5mM) was dissolved in acetonitrile and dichloromethane. To it was added 100 µM (4 equivalents) of ceric ammonium nitrate (precooled at -40°C) and the UV-Vis and HRMS was recorded immediately.

Kinetic Isotope Effect Analysis

The KIE was studied in 0.1M deuterated buffer (pD = 9.2) and protonated buffer (pH = 9.2). The pH of the deuterated buffer was measured by pH meter to be 8.8. To obtain the exact pD value, 0.4 was added to the pH meter reading.[6] The shift in the pK_a of the protonable groups is about the same value, since the protonation level of these groups is almost the same as in H_2O and D_2O respectively, at the same pH meter reading.

Details of electrochemical Kinetics analysis

Kinetic rate constants for diffusion limited WO were determined from the CV experiments. The catalytic current (i_{cat}) for a second-order reaction is given by eq. 1, where n_{cat}, F, A, [Co], D, k_{cat} are the number of electron transported during catalytic reaction (n = 4 for water oxidation), the Faraday constant, electrode area, catalyst concentration, the diffusion coefficient, second-order rate constant respectively.

$i_{cat}= n_{cat} FA[Co]D^{1/2}k_{cat}^{1/2}[H_2O]^{1/2}= n_{cat} FA[Co]D^{1/2}k_{obs}^{1/2}$ …………………(1)

The second order rate constant k_{cat} is correlated with the first order catalytic rate constant, k_{obs}, by eq. 2 under pseudo first-order conditions.

$k_{obs}= k_{cat}[H_2O]$ ……………… (2)

The current at the anodic peak potential ($E_{p,a}$) is calculated from the Randles-Sevcik equation[7] (equation 3),where n_{cat}, n, v, R, T are the number of electron transferred during WO, scan rate of voltammetry, universal gas constant, and temperature respectively. Here n =

1, no of electron transfer per catalyst in redox wave (where catalysis is not involved) and n_{cat} = 4, no of electron required to evolve one molecule of oxygen during WO.

$$i_P = 0.446nFA[\text{Co}]\sqrt{\frac{nFvD}{RT}} \quad \text{..(3)}$$

Dividing equation 3 by equation 1 provides equation 4.

$$\frac{i_{cat}}{i_p} = \frac{n_{cat}\sqrt{RT}k_{obs}^{1/2}}{n^{3/2}0.446\sqrt{F}v^{1/2}} = \frac{n_{cat}\sqrt{RT}k_{cat}^{1/2}[\text{H}_2O]^{1/2}}{n^{3/2}0.446\sqrt{F}v^{1/2}} \quad \text{...................(4)}$$

Background corrected ratio of i_{cat} and i_p was plotted as a function of the inverse of the square root of scan rate. A linear fit (y = 3.41x) with zero intercept between i_{cat}/i_p and square root of scan rate results a slope (m= 3.41). From this slope rate constants for WO were determined.
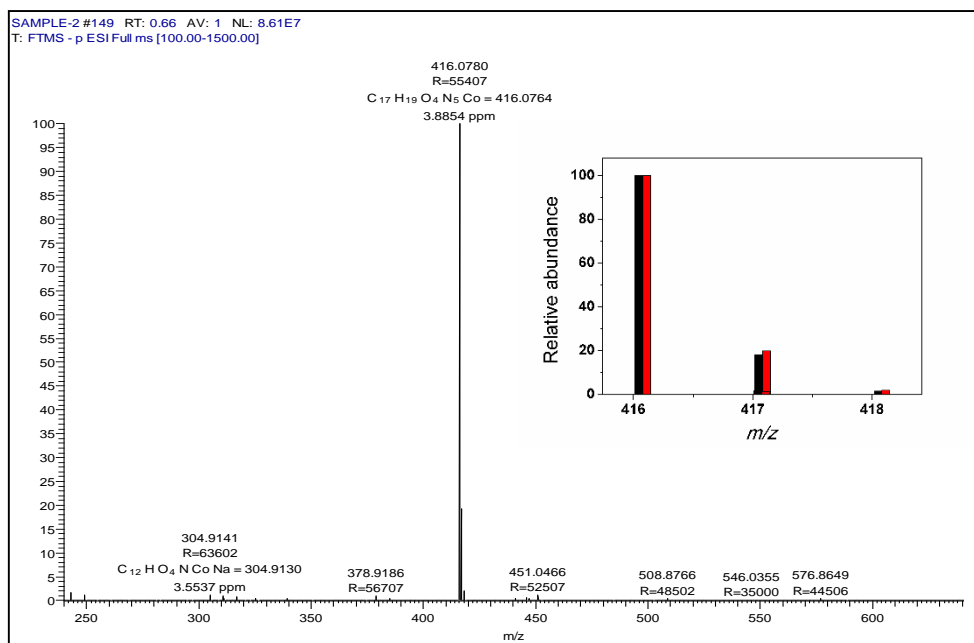
Figure S1. High resolution mass spectrum of (Et$_4$N)[Co^{III}-bTAML] (2) in CH$_3$CN (observed *m/z* 416.0780, calculated for C$_{17}$H$_{19}$O$_4$N$_5$Co *m/z* 416.0764). Inset shows comparison of simulated (red bars) and observed (black bars) isotopic distribution pattern for ion of interest ("3.8854 ppm" represents resolution and the number refers to the error associated with the experiment).
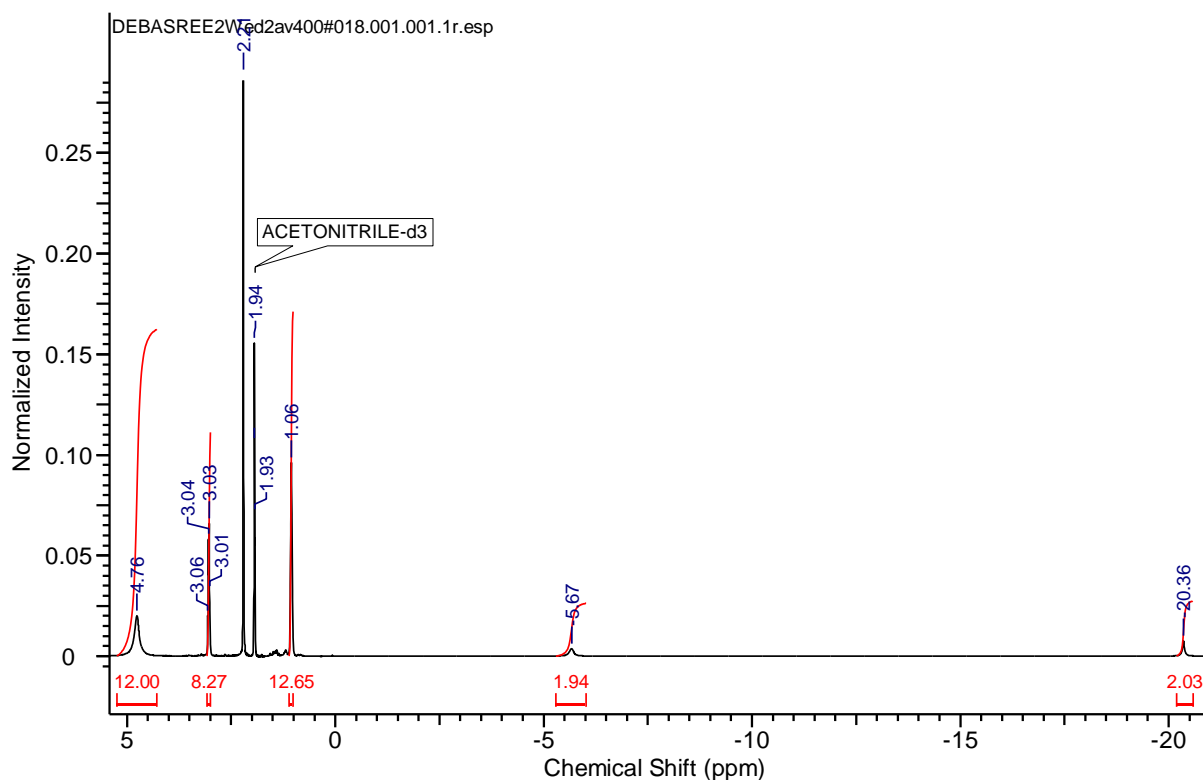
Figure S2. ^{1}H NMR of (Et$_4$N)[Co^{III}-bTAML] (**2**) in CD$_3$CN (400MHz, 25^{0}C).
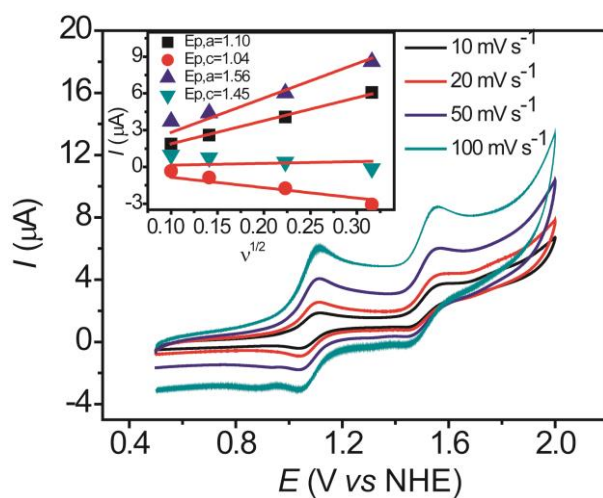
Figure S3. CVs of 0.5 mM **2** in acetonitrile (0.1 M potassium hexafluoro phosphate as the supporting electrolyte) at room temperature with varying scan rates. Inset shows $I_{p,a}$ and $I_{p,c}$ for two redox couple at different scan rates *vs* the square root of scan rate.
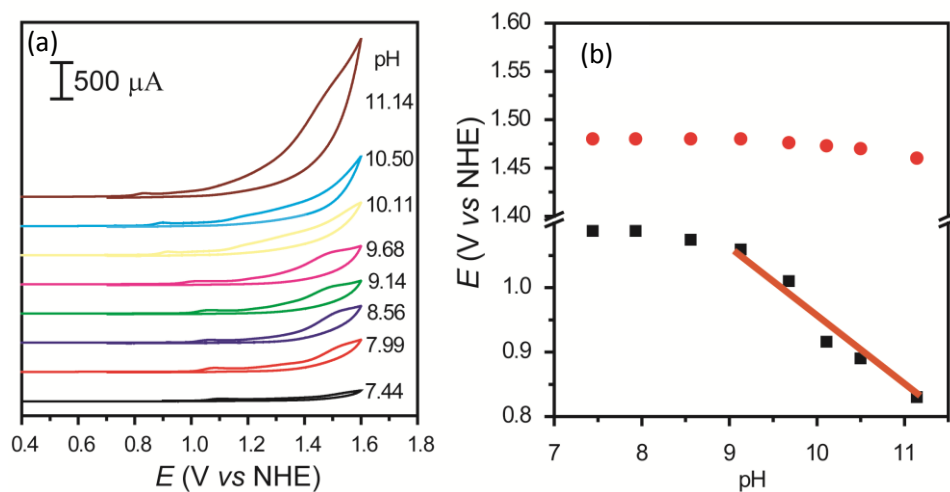
Figure S4. (a) CVs of 0.5 mM (EtN$_4$)[Co^{III}(b-TAML)] (**2**) at 100mV/s scan rate in 0.1M phosphate buffer at different pH. (b) Plots of first (black circles) and second (red circles) anodic peak potential *vs* different pH. The red line indicates linear fit from pH 9 to pH 11 with a slope of 118mV.
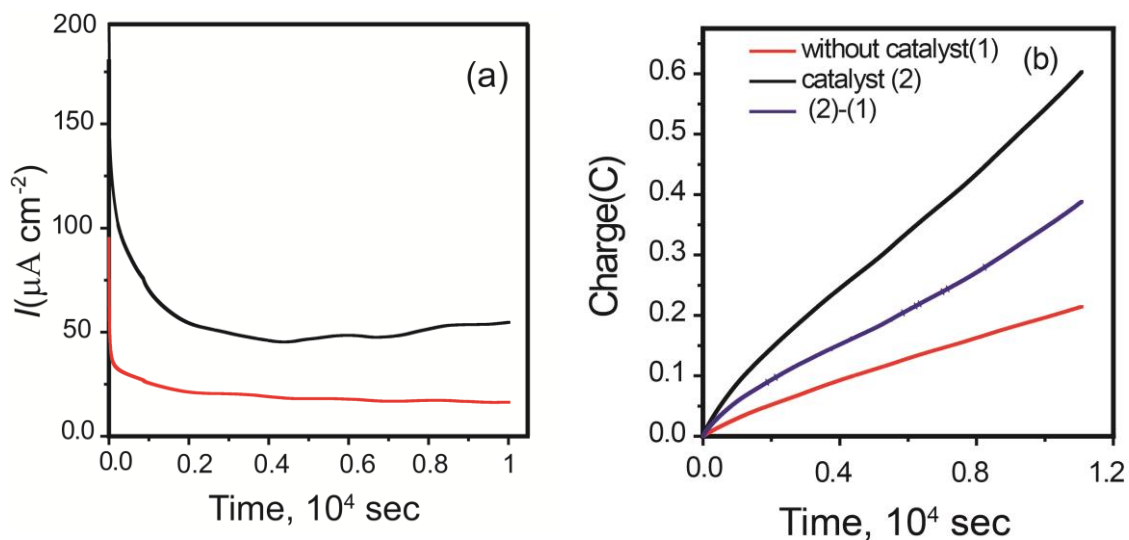
Figure S5. (a) Current obtained and (b) charge passed in 3 hours with 1mM **2** (black line) and without **2** (red line) during CPE at 1.5 V (*vs* NHE) in pH = 9.2 phosphate buffer (0.1 M) on 1 cm² clean ITO surface (condition: platinum wire as counter electrode and Ag/AgCl (saturated KCl as reference electrode)).
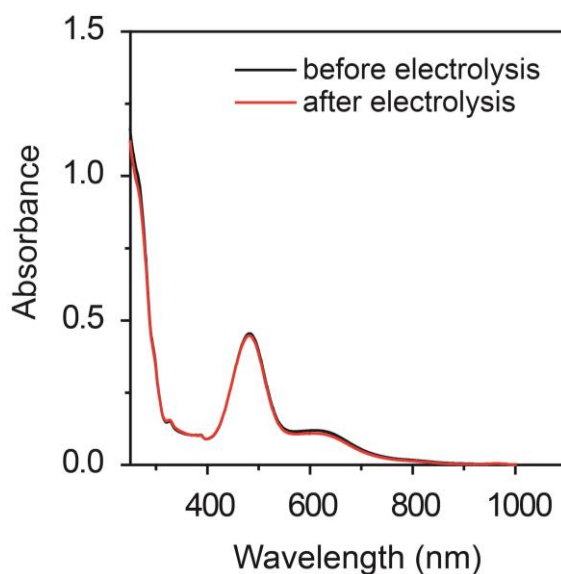
Figure S6: UV-Visible spectra of 0.1 mM **2** in water (0.1M pH = 9.2 phosphate buffer) before (black) and after (red) 3 hours of CPE.
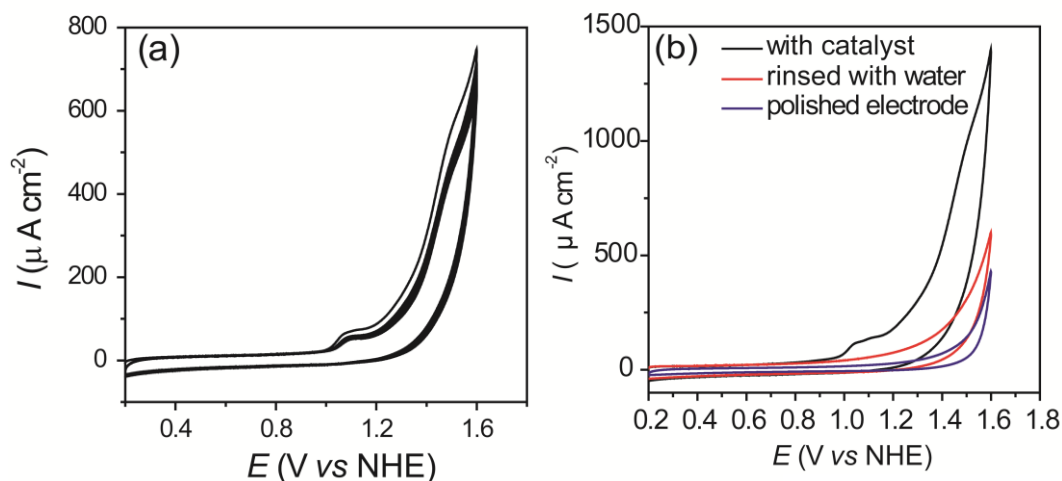
Figure S7. (a) CV of twenty continuous scan cycles of 0.25 mM **2** in 0.1M phosphate buffer (pH = 9.2) at 100mV/s scan rate. (b) After twenty continuous scan cycles the GC electrode was taken out from the solution and washed carefully with only deionized water. The washed GC electrode (unpolished) was then cycled in fresh 0.1 M phosphate buffer (pH = 9.2) (scan rate 100mV/s) solution without catalyst. CVs of (i) 0.25 mM **2** (black) (ii) rinsed GC electrode (not polished) (red) (iii) polished GC electrode in the 0.1M phosphate buffer (pH = 9.2) (scan rate 100mV/s).
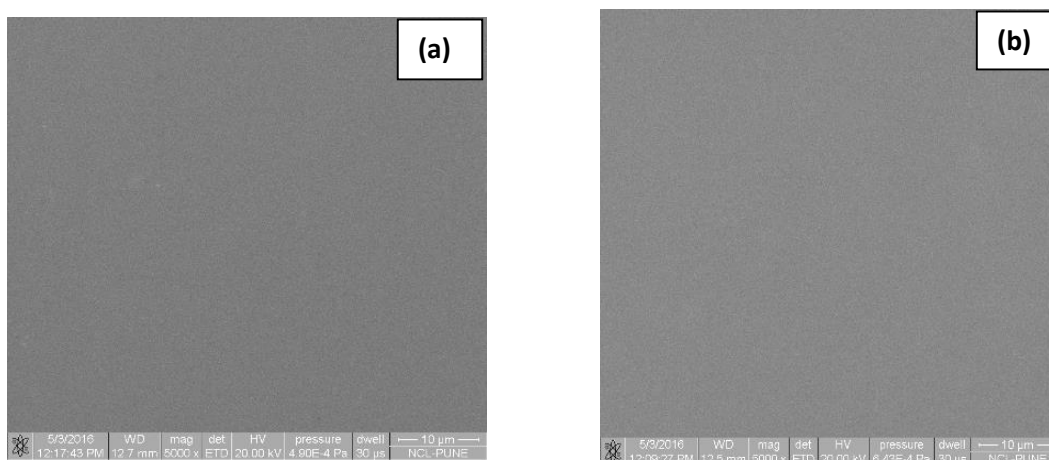
Figure S8. Scanning electron microscopy (SEM) images of a ITO working electrode before (a) and after (b) 3 hours of CPE at pH = 9.2 phosphate buffer.
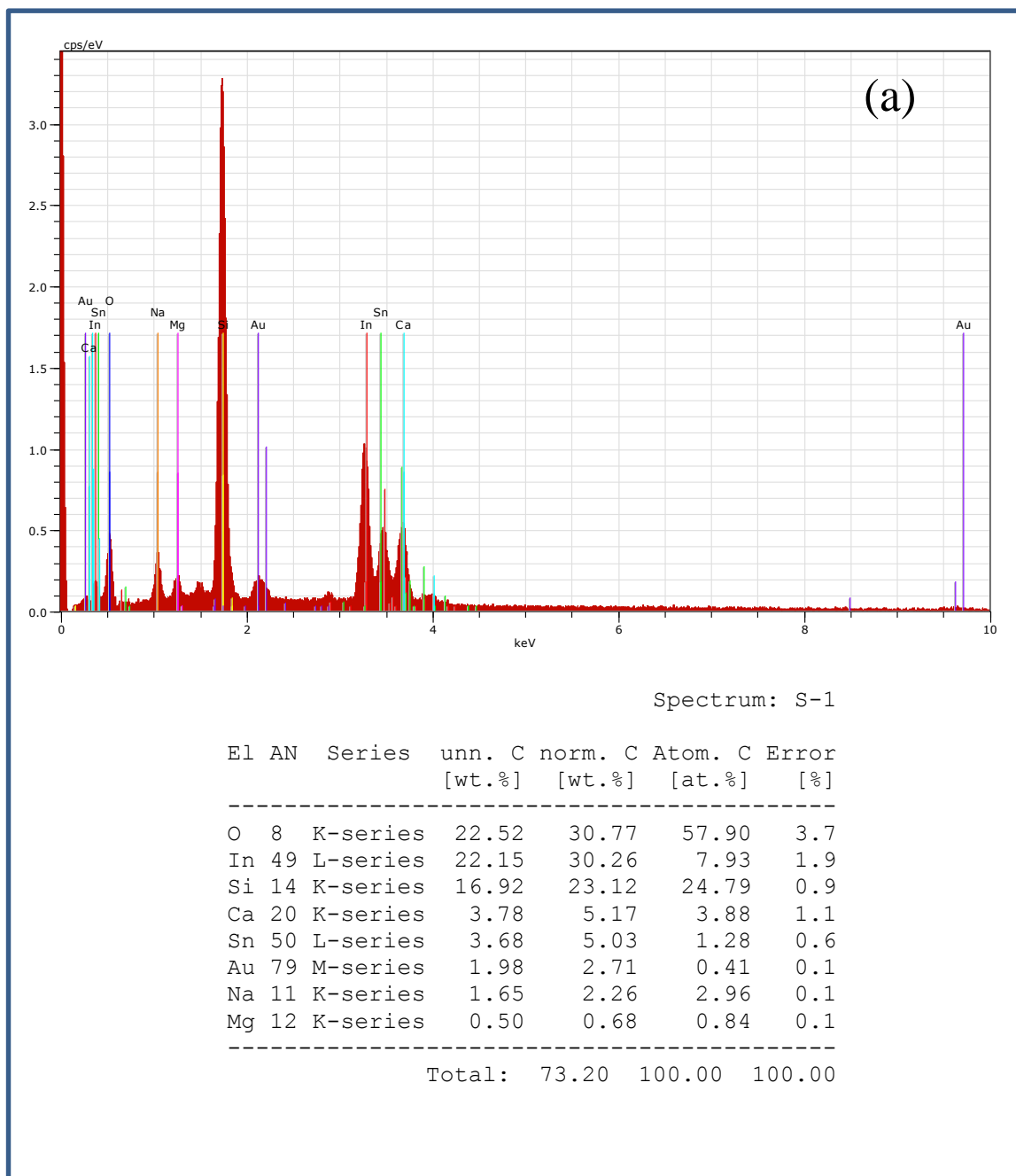
Figure S9a. Energy dispersive X-ray analysis (EDX) of a clean ITO electrode before CPE (the above table indicates the composition ITO electrode surface).

```
Spectrum: S-2

El AN   Series   unn. C  norm. C  Atom. C  Error
                 [wt.%]   [wt.%]   [at.%]    [%]
---------------------------------------------------
In 49  L-series   23.41    32.35     8.76    2.0
O   8  K-series   20.70    28.60    55.58    3.6
Si 14  K-series   17.11    23.65    26.17    1.0
Ca 20  K-series    4.08     5.64     4.37    1.2
Sn 50  L-series    3.59     4.95     1.30    0.6
Au 79  M-series    1.57     2.17     0.34    0.1
Na 11  K-series    1.35     1.86     2.52    0.1
Mg 12  K-series    0.40     0.56     0.72    0.1
Al 13  K-series    0.15     0.21     0.25    0.0
---------------------------------------------------
       Total:     72.36   100.00   100.00
```
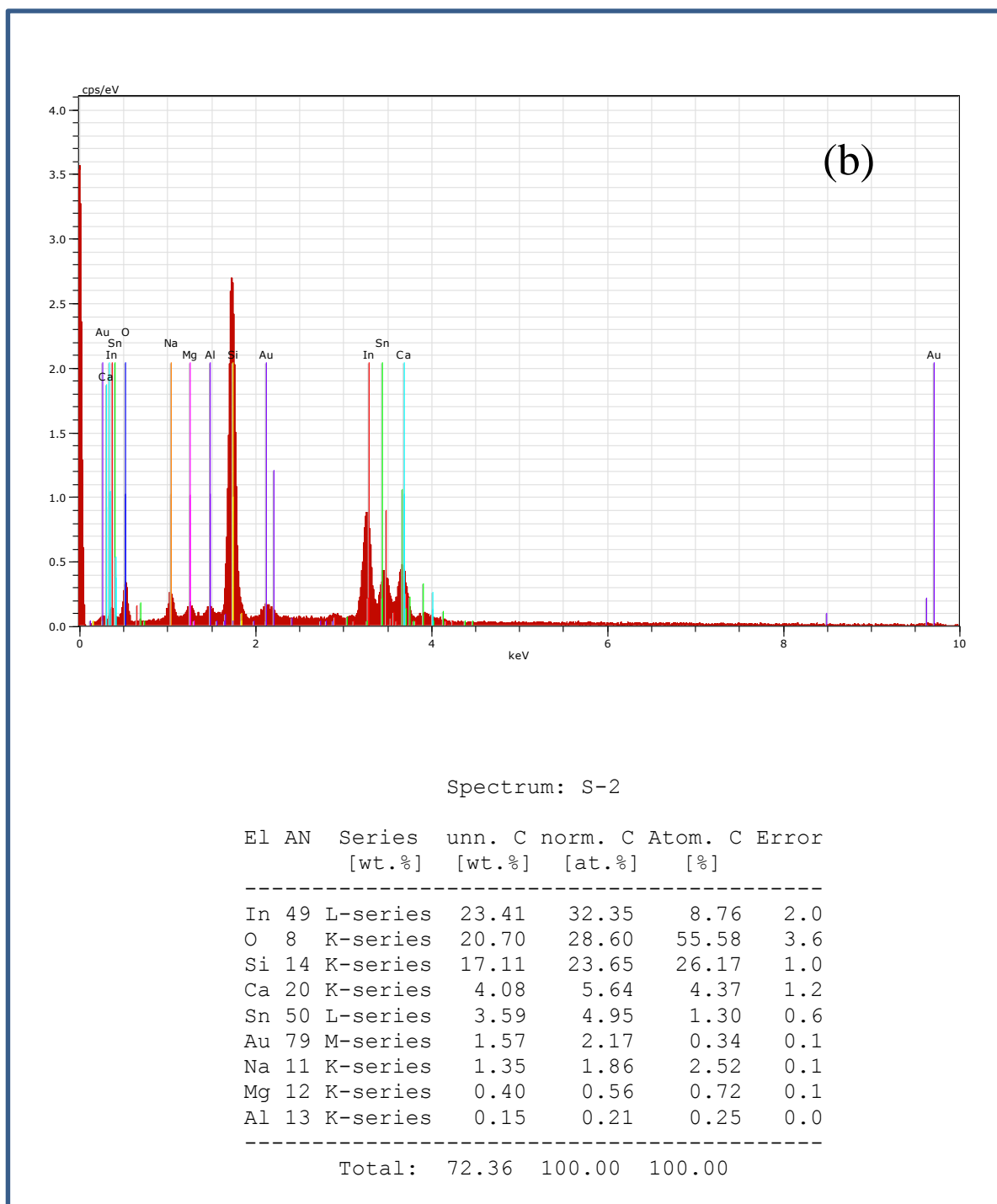
Figure S9b. Energy dispersive X-ray analysis (EDX) of a ITO electrode after CPE (the above table indicates the composition of the ITO electrode surface).

```
--------------------------------------------------------------
Initialisation
--------------------------------------------------------------

Setting temperature to 25.0°C...

Equilibrating sample for 120 seconds...

--------------------------------------------------------------
Size measurement
--------------------------------------------------------------

Starting measurement 1

90 degree measurement

--------------------------------------------------------------
Optimisation
--------------------------------------------------------------

Checking preset position

Seeking best attenuator at position 4.65mm...
Set attenuator: 11
Count rate: 0.88 kcps
Unable to find a suitable attenuator. Count rate is too low for acceptable measurement.

[ATTENTION]: Unable to find an optimum attenuator and measurement position.
[ATTENTION]: Low count rate
Measurement aborted

Setting temperature to 25.0°C...
```

Figure S10. Report of dynamic light scattering (DLS) experiment for catalyst **2** in 0.1M phosphate buffer (pH = 9.2) after 3 hours of CPE.
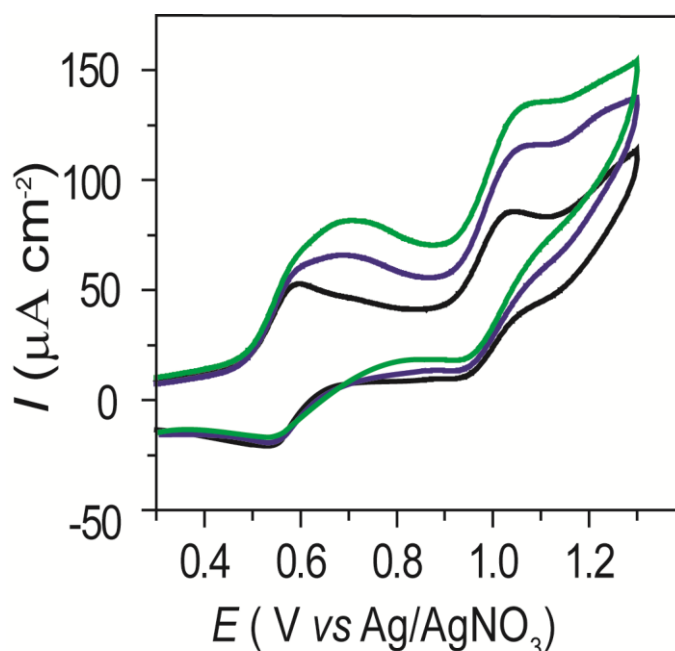
Figure S11. CVs of **2** (0.5mM) in (black) acetonitrile, 0.4 % pH 9.2 (0.4 mM phosphate buffer) in acetonitrile (blue) and 0.5 % pH =9.2 0.5 mM buffer in acetonitrile (green). Conditions: Scan rate 50 mVs^{-1}, Glassy carbon as working electrode, platinum wire as counter electrode, Ag/AgNO$_3$ as reference electrode and 0.1 M potassium hexafluoro phosphate as supporting electrolyte.
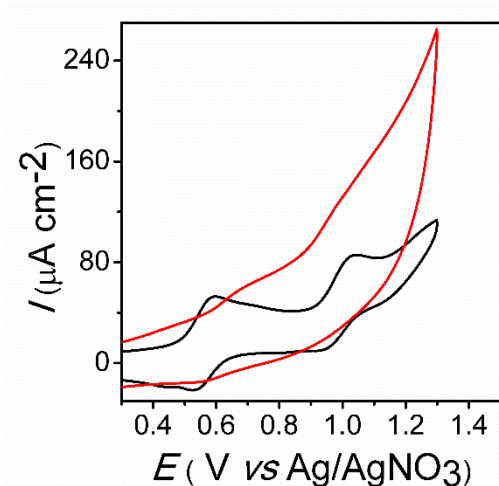
Figure S12. CVs of **2** in acetonitrile (black); acetonitrile:1.75 % pH 9.2 (0.1M phosphate buffer) (red). Conditions: scan rate 50mV/s, glassy carbon as working electrode, platinum wire as counter electrode, non aqueous Ag/AgNO₃ as reference electrode and 0.1 M potassium hexafluoro phosphate as supporting electrolyte.
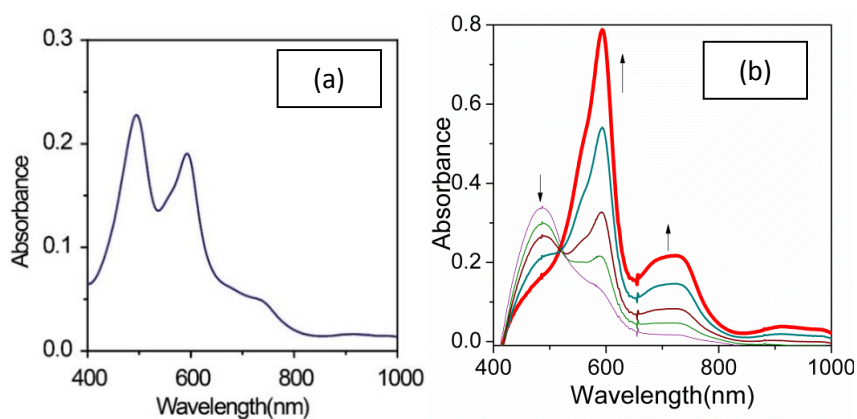
Figure S13. (a) UV-Vis spectrum of mixture of $[Co^{IV}(O)bTAML]^{2-}$ and $[Co^{III}\text{-}bTAML]^{-}$ generated by controlled potential electrolysis (1.2 V *vs* NHE) in acetonitrile at -15⁰C. (b) Conversion of **2** to one electron higher oxidized species $[Co^{IV}(O)bTAML]^{2-}$ through isosbestic point at 510 nm by CPE at -15⁰C. Condition: 9 cm² clean ITO as working, platinum foil as counter, Ag/AgNO₃ as reference electrode and 0.1 M potassium hexafluoro phosphate as supporting electrolyte.
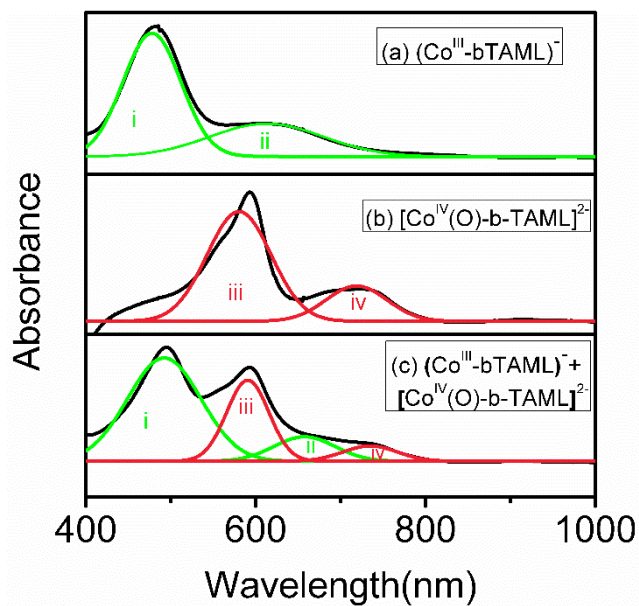
Figure S14. Absorption spectra of (a) [Co^{III}-bTAML]$^-$, (b) [Co^{IV}(O)bTAML]$^{2-}$ (c) mixture of [Co^{IV}(O)bTAML]$^{2-}$ and [Co^{III}-bTAML]$^-$. The spectra in (a) to (c) have been fitted to sums of Gaussian functions , and the component bands are assigned as i , ii, iii, iv.
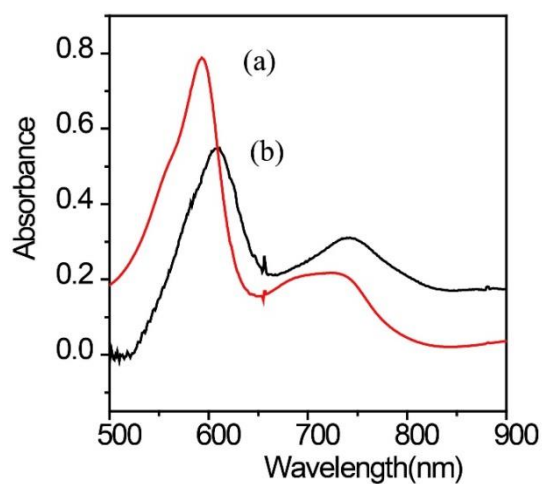
Figure S15. UV-Vis spectra of complex [Co^{IV}(O)bTAML]$^{2-}$ in (a) acetonitrile and (b) dichloromethane generated from **2** by addition of chemical oxidant (ceric ammonium nitrate) at -40^{0}C.
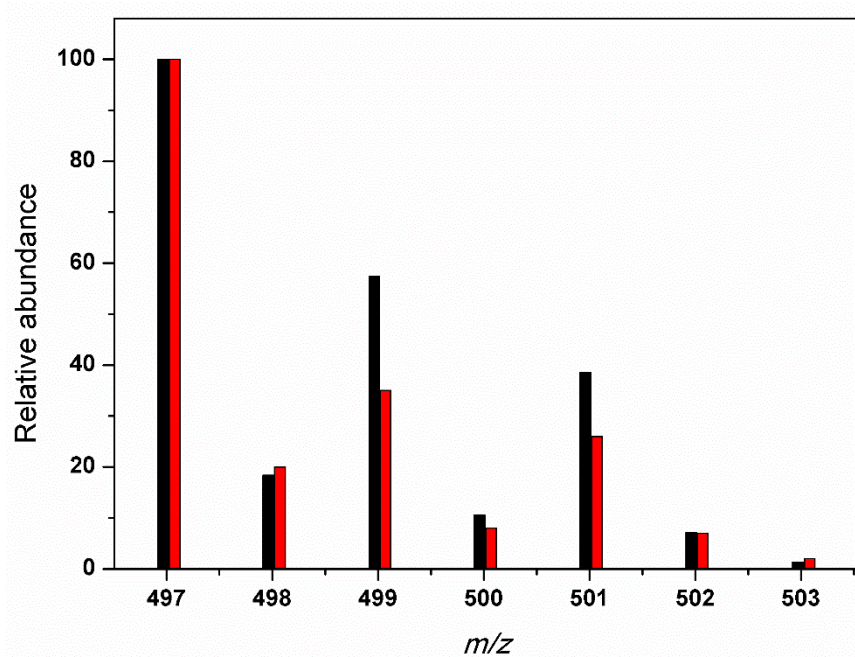
Figure S16. Comparison of simulated (black bars) and observed (red bars) isotopic distribution pattern of $[Co(O)(Zn)(bTAML)]^-[H]^+$

Table 1: Crystal data and structure refinement for [Co^{III}-bTAML]$^-$

Identification code	Co-TAML
Empirical formula	C25 H39 Co1 N6 O4
Formula weight	546.55
Temperature/K	298
Crystal system	monoclinic
Space group	P2$_1$/n
a/Å	14.5396(10)
b/Å	9.6307(6)
c/Å	20.8295(15)
α/°	90.00
β/°	109.316(8)
γ/°	90.00
Volume/Å^3	2752.5(3)
Z	4
ρ_{calc}mg/mm^3	1.319
m/mm^{-1}	0.664
F(000)	1160.0
Crystal size/mm^3	0.4 × 0.2 × 0.2
2Θ range for data collection	5.92 to 58.46°
Index ranges	-18 ≤ h ≤ 18, -13 ≤ k ≤ 13, -28 ≤ l ≤ 27
Reflections collected	16350
Independent reflections	6537[R(int) = 0.0871]
Data/restraints/parameters	6537/0/334
Goodness-of-fit on F^2	1.069
Final R indexes [I>=2σ (I)]	R$_1$ = 0.0816, wR$_2$ = 0.2206
Final R indexes [all data]	R$_1$ = 0.1348, wR$_2$ = 0.3008
Largest diff. peak/hole / e Å^{-3}	0.596/-0.860

References:

1 CrysAlisPro, Version 1.171.33.66; Oxford Diffraction Ltd.: Abingdon, U.K., 2010.

2 G. M. Sheldrick, (1997). SHELXS '97 and SHELXL '97. University of Göttingen, Germany

3 A. L. Spek (2005) PLATON, A Multipurpose Crystallographic Tool, Utrecht University, Utrecht, The Netherlands.

4 W. L. F. Armarego, C.L.L. Chai, *Purification of Laboratory Chemicals, 5th ed*. Elsevier Science: Burlington, MA, 2003.

5 C. Panda, M. Ghosh, T. Panda, R. Banerjee and S. Sen Gupta, *Chem. Commun*., 2011, **47**, 8016–8018

6 S. Chatterjee, K. Sengupta, S. Samanta, P. K. Das, and A. Dey, *Inorg. Chem.* 2015, **54**, 2383–2392.

7 A. J. Bard and L. R. Faulkner, *Electrochemical Methods: Fundamentals and Applications*, John Wiley & Sons, Inc.: New York, 2001.